

Digital microfluidic chip technology for water permeability measurements on single isolated plant protoplasts

Phalguni Tewari Kumar ^a, Federica Toffalini ^a, Daan Witters ^a, Steven Vermeir ^a, Filip Rolland ^b, Maarten L.A.T.M. Hertog ^a, Bart M. Nicolai ^{a,c}, Robert Puers ^d, Annemie Geeraerd ^a and Jeroen Lammertyn ^{*a}

^a KU Leuven – University of Leuven, BIOSYST-MeBioS, Willem de Croylaan 42, Leuven, Belgium.

^b KU Leuven – University of Leuven, Laboratory of Molecular Plant Biology, Kasteelpark Arenberg 31, Leuven, Belgium

^c Flanders Centre of Postharvest Technology – Willem de Croylaan 42, Leuven, Belgium

^d KU Leuven – University of Leuven, MICAS-ESAT, Kasteelpark Arenberg 10, Leuven, Belgium

* Corresponding author at: KU Leuven – University of Leuven, BIOSYST-MeBioS, Willem de Croylaan 42, Leuven, Belgium. Phone: +32 16 3 21459; Fax: +32 16 3 22955; E-mail: jeroen.lammertyn@biw.kuleuven.be

Abstract

Dynamic follow up and analysis of isolated single cells that display non-adhering behaviour is hindered by the fact that they float in the suspension medium and thus requires the implementation of systems that physically entrap the cells for successful analysis. We describe the potential of digital microfluidic (DMF) chip technology for conducting analysis of cells in suspension at the single cell resolution. More specifically, we demonstrate the use of DMF technology for the analysis of a group of single individual protoplasts from *Arabidopsis thaliana* plants that are labelled with magnetic particles and are immobilized on the DMF chip by magnetic forces. By transporting droplets with different osmotic conditions to the site where the cells are trapped, we challenge the cells and monitor their responses dynamically with a camera. The use of DMF technology for performing water potential measurements has the following advantages: (i) solid particles such as cells and magnetic beads are manipulated on the chip without the risk of clogging channels, (ii) low shear stress during droplet unit operations like mixing and transport that characterize DMF are particularly suited for analysis of delicate cells types that lack cell walls such as protoplasts, (iii) the throughput of the analysis is strongly increased as multiple protoplasts are analysed simultaneously, in contrast with the traditional methods that can handle and challenge only one cell at a time. We show that the DMF analysis platform is effective in creating the steep osmotic gradients required for calculation of water permeability coefficients (P) as the values found are comparable with previously reported ones thus validating the suitability of the technology for such studies. This work illustrates a proof of concept for the applicability of DMF as an unparalleled and promising system for implementing single cells studies on non-adhering cells in an automated way.

Keywords: Digital microfluidic chip; Water permeability coefficient; Protoplasts; Magnetic cell immobilization; Single cell analysis; Lab-on-a-chip

1. Introduction

Absorption of water molecules and solutes from the environment and their transport in plants represents one of the

oldest subjects in plant physiology. Water relation studies investigate the movement of water and solute molecules across semi-permeable plasma membranes that separate solutions with different osmotic potentials. Until the discovery of aquaporins, it was believed that water movement due to the osmotic gradients was the result of simple diffusion of molecules through the lipid bilayer and that variations existed in the permeability of plasma membranes due to different lipid compositions [1]. The discovery of aquaporins as regulatory channels that facilitate the transmembrane movement of water, shed new light onto the mechanism of water transport and led to the conclusion that each semi-permeable membrane is characterized by a certain water permeability, which is strictly linked with the level of expression and activity of aquaporins [2]. Activity and number of aquaporins present in the plasma membrane significantly influence the regulation of water transport in cells [3], which also depends on cell type and organ [4]. From a mathematical point of view, the permeability of a membrane can be expressed in terms of the water permeability coefficient (P) which is a measure of the flux at which water flows through the membrane. A number of studies have investigated water transport in plants, both at the whole plant and tissue level. Traditionally, pressure chambers [5] and pressure probes [6,7] have been used to measure osmotic potentials of whole tissues or of cells within a certain tissue. Water relation studies have also been performed on single isolated cells, typically protoplasts, by exposing cells to a sudden osmotic pressure change and then calculating the P values [8]. In such experiments protoplasts are treated with hyper- or hypotonic solutions and the altered osmotic environment drives water movement across plasma membrane. The water taken up or released by the protoplasts results in volume changes that are monitored with an external camera and are used to calculate the P value [8,9]. It is evident that accurate volume measurement and subsequent P calculation strongly depends on efficient immobilization of the cell to be monitored during the re-equilibration phase. Unlike adherent animal cells, which have a natural tendency to adhere on certain surfaces and retain this property after isolation from the organ or tissue of origin, plant cells remain in solution as suspended particles upon isolation, adding an extra layer of complexity to the proper execution of P measurements. Researchers have overcome this limitation by using tools such as micropipettes [9] and micromanipulators [10] that can hold a cell in place during rapid solution exchange. Although a very effective approach, manual handling of only one cell at a time significantly compromises the throughput in this type of analysis. Immobilization of protoplasts with a suction micropipette has also several conceptual disadvantages such as no uniform exposure of the cell surface to the changed environment, potential distortion of the cell shape and mechanical disturbance of the membrane integrity [11]. Recently optical tweezers (OT) have proven to be an effective manipulation tool for trapping naturally non-adhering cells using highly focussed near infrared beams [12,13]. Major challenges for using OT as trapping method are parallel manipulation of cells comprising of inhomogeneous sizes. Also for conducting physiological studies where size may change over time, OT will provide low throughput due to a constant optimization of the laser. Lastly, careful exposure to the laser beam is essential to avoid photo-damage of cells [14]. It has become apparent that novel approaches are needed to increase the throughput of these types of studies on plant cells while preserving the high potential of performing the analysis at the single cell level.

Since almost a decade, microfluidics has been looked upon as a promising alternative for conducting cell based studies in a miniaturized and automated manner. A digital microfluidic (DMF) chip is a two-plate system in which the bottom plate carries a planar array of electrodes that can be individually activated in a software-assisted manner,

76 whereas the top plate acts as a ground electrode. Discrete reagent droplets sandwiched between the two plates are
77 transported across the electrode array by using the electrowetting on dielectric (EWOD) actuation principle.
78 For specific cell-based applications, DMF chips have unique advantages that make them a preferable choice over
79 other types of microfluidic systems. Besides reduced reagent and sample consumption, and waste creation, DMF
80 chips feature low shear stress during droplet unit operations like mixing and transporting, which is particularly
81 important when dealing with cell types that are particularly sensitive to physical stress such as cells devoid of a cell
82 wall. As droplet movement occurs on arrays of electrodes and signals are generated with software controlled
83 electrical signals, droplet movement is highly reconfigurable between different experimental setups. But arguably the
84 most exclusive advantage of DMF, especially in comparison with microchannel-based devices, is its exquisite
85 control of suspended solids that, by being transported over open planar surfaces, cannot cause clogging of channels.
86 In DMF, solids particles are transported using a receding droplet meniscus, a mechanism that has also been used for
87 depositing solids at dedicated spots where they are geometrically trapped or molecularly bound [15].

88 DMF technology has already been proven suitable and effective for the implementation of cell culture and cell
89 based assays in several systems using naturally adhering cell types [16,17]. Complete mammalian cell culture and
90 transfection were implemented on a DMF chip where the nutrient medium and all the transfection reagents were
91 delivered by transporting droplets across the platform [18]. Recently, an optoelectronic tweezers integrated digital
92 microfluidic device was demonstrated for manipulating a group of HeLa cells [19]. Although the work was a proof
93 of concept and was successfully demonstrated for multiple cells, the task was challenging as reported by the authors
94 and the system itself required thorough optimization. In other work, an apoptosis assay was implemented on
95 adherent cells to demonstrate the potential of DMF chips for performing multiplexed assays with reduced reagent
96 consumption and lower detection limits than traditional methods [20]. All these examples feature the creation of
97 adhesion patches within the hydrophobic chip surface to which cells naturally adhere. On the other hand,
98 applications of DMF with non-adherent cell types have remained at the present less explored. Examples of this type
99 of applications include a microbial bioreactor where populations of bacterial, algae and yeast cells were cultured on-
100 chip with automated semi-continuous mixing [21]. A few examples are available where cell based assays on cells in
101 suspension have been demonstrated [22]. For example, cells were treated with certain cytotoxic reagents and the cell
102 response in terms of viability was monitored using intracellular staining. To the best of our knowledge, the use of
103 DMF chips for analysis of cells in suspension at the single cell resolution still remains unreported in literature,
104 probably due to the challenge of physically constraining single cells at defined locations on the chip surface.

105 Here we report for the first time a method based on DMF chips that automates the osmotic treatment of a group of
106 isolated single protoplasts immobilized on the chip surface through magnetic bead labelling. The described
107 immobilization strategy bypasses the need for external devices to hold cells in place during buffer exchange. As
108 compared to optical tweezers, this strategy is easily applicable on a batch of cells with mixed sizes for conducting
109 physiological studies with a high throughput. We demonstrate that this DMF-based system is suitable and effective
110 for the measurement of water permeability coefficients at the single cell level with substantial increase of the
111 throughput as groups of several protoplasts can be treated and monitored simultaneously. This work offers an
112 automated and versatile solution for all those types of analyses that require monitoring of single cells that are
113 naturally non-adhering to a substrate yet at the single cell resolution.

2. Materials and Methods

2.1 Reagents

4-morpholineethanesulfonic acid (MES), bovine serum albumin (BSA), mannitol, CaCl_2 and KCl were purchased from Sigma Aldrich (Oakville, ON, USA). Cellulase R10 was purchased from Yakult Pharmaceutical Ind. Co., Ltd., Japan and Macerace™ Pectinase, *Rhizopus* sp., was purchased from Merck. All above solutions were filter-sterilized using a 0.45- μm filter. Biotinylated concanavalin A (ConA) was purchased from Vector Laboratories (Burlingame, CA, USA) and was dissolved in water. Streptavidin coated magnetic microparticles (MMP) (M-280 Dynabeads) were obtained from Life Technologies (Carlsbad, CA, USA). Reagents used for photolithography included S1818 and 351-developer (Rohm and Haas, Marlborough, MN, USA). Parylene-C dimer was purchased from Plasma Parylene Coating Services (Rosenheim, Germany), and Teflon-AF® was obtained from Dupont (Wilmington, DE, USA).

2.2 Protoplast Isolation

Protoplasts were isolated from 5 weeks old *Arabidopsis thaliana* L. plants (ecotype Columbia; grown at a 12h/12h day/night regime, 75 μE) with fully expanded 2nd or 3rd pair true leaves as described in literature [23]. Essentially, 10 mL of enzyme solution (0.4 M mannitol, 20 mM KCl, 20 mM MES buffer pH 5.7, 1.5% cellulase and 0.4% pectinase) was first incubated at 55°C for 10 min and put on ice for 10 min. Next, 10 mM CaCl_2 and 0.1% BSA were added to the solution which was then filter-sterilized using a 0.45 μm filter into a Petri dish. About 15 striped leaves were then added to the enzyme solution and vacuum infiltrated for about 30 min in the dark. Finally, the enzyme solution was incubated in the dark for an additional 2.5 h followed by the addition of an equal amount of W5 buffer (154 mM NaCl, 125 mM CaCl_2 , 5 mM KCl and 2 mM MES buffer). The resulting solution was filtered through a nylon mesh (pore size 35-75 μm) in a round bottom tube and the filtrate was concentrated in a centrifuge with swinging buckets at 200 g (Hettich Zentrifugen, Universal 30RF, Germany). The pellet was then dissolved in 1 mL W5 buffer and the protoplast viability was assessed by morphological examination under a microscope (BX40-Olympus, Japan). The number of protoplasts was counted on a haemocytometer and the cell concentration was finally adjusted to 2.5×10^5 cells/mL.

2.3 Magnetic microparticle (MMP) labelling of protoplasts

The general procedure is summarised in Fig. 1(a-c). Protoplasts (Fig. 1a) were first conjugated with biotinylated ConA which specifically binds to the α -linked mannose groups present on their plasma membrane and results in the exposure of biotin groups on the cell surface (Fig. 1b). Next, ConA conjugated protoplasts were incubated with streptavidin coated MMP allowing high affinity binding between the exposed biotin groups and the streptavidin molecules (Fig. 1c). This technique has been previously reported in literature [24–26] for the isolation of cells and plasma membrane proteins and is applied here for the immobilization of single protoplasts on the DMF chip.

2.3.1 ConA functionalization: 0.5 mL of protoplast suspension was incubated with ConA in the dark in a 1.5 mL microcentrifugation tube at the indicated final concentration. The solution was then allowed to mix on a rotator

mixer (PTR-30, Grant Bio, England) for 40 min. Cell number was then determined using a counting chamber and the number of protoplasts that burst during the procedure was expressed as a percentage of the initial number of protoplasts.

2.3.2 MMP-protoplast conjugation and isolation: The solution containing ConA functionalized protoplasts was centrifuged at 196 g for 2 min and the pellet was dissolved in 0.5 mL W5 buffer. Protoplasts were then incubated with MMP at the indicated final concentration in a microcentrifugation tube in the dark and allowed to conjugate on a rotator mixer for 40 min. The MMP-bound protoplasts were isolated from unbound protoplasts with a magnetic particle concentrator (DynaL MPC®-S, Life technologies, California). After three washing steps, MMP labelled protoplasts were suspended in 100 µL W5 buffer and used in DMF chip experiments.

2.4 Chip fabrication and operation

DMF chips were fabricated in the ESAT-MICAS cleanroom facility of the University of Leuven as previously described with some minor modifications [27]. In summary, cleaned glass wafers (1.1 mm thickness) were sputter coated with chromium (100 nm) and patterned using standard photolithographic processes. Next, chips were cleaned in O₂-plasma (150 mtorr, 100 W) and primed with silane A174 before being coated with a layer of Parylene-C (3 µm) using chemical vapour deposition. A thin layer of Teflon-AF® (~200 nm thickness, 3% w/w in Fluorinert FC-40) was subsequently spincoated (1200 rpm) on top of the Parylene-C layer, baked for 5 min at 110°C and 5 min at 200°C. Crenelated actuation electrodes of 2.8 mm × 2.8 mm were used for the manipulation of individual droplets of 4.5 µL volume. In addition to the conventional bottom electrode layout, visualization windows were fabricated for monitoring cells using an inverted microscope. The top plate of the DMF device was fabricated by spincoating Teflon-AF® (as above) on top of indium tin oxide-coated glass slides (Delta technologies Ltd, Stillwater, MN, USA). Tape of 160 µm thickness was applied on the bottom plate as a spacer before assembling the double-plate microfluidic device. A chip holder was designed and custom-made for actuating the DMF device and for allowing visualization from the bottom side of the chip. The actuation sequence of electrodes was controlled with a customised Labview program (National Instruments Corp., Austin, TX, USA) and an in-house developed Matlab program (MathWorks Inc., Natick, MA, USA). Droplets were driven by an AC-voltage of 120-130 V_{rms}, an activation time of 1000 ms and a relaxation time of 40 ms. AC-actuation voltage was realized by the oscillating waveforms, produced by the function generator operating at 1 kHz (GFG-8216A-ISO-TECH, England), that were further amplified by an amplifier (FLC Electronics A600, Origin Sweden).

2.5 Water potential measurements and image analysis of protoplasts

To perform the water permeability measurements, the DMF bottom plate was encased in the chip holder for electrical connections and a droplet of 4.5 µL containing MMP-bound protoplasts (-1.6 MPa, corresponding to the intrinsic osmotic pressure) was manually dispensed on the bottom plate above the electrode containing a visualization window. A second droplet containing ultrapure water (3.2 or 6.5 µL for a resulting osmotic pressure change of 0.99 or 0.70 MPa, respectively) was also dispensed on another electrode of the bottom plate. The top plate was then placed on top of the bottom plate in the DMF holder and a magnetic field was applied through an external

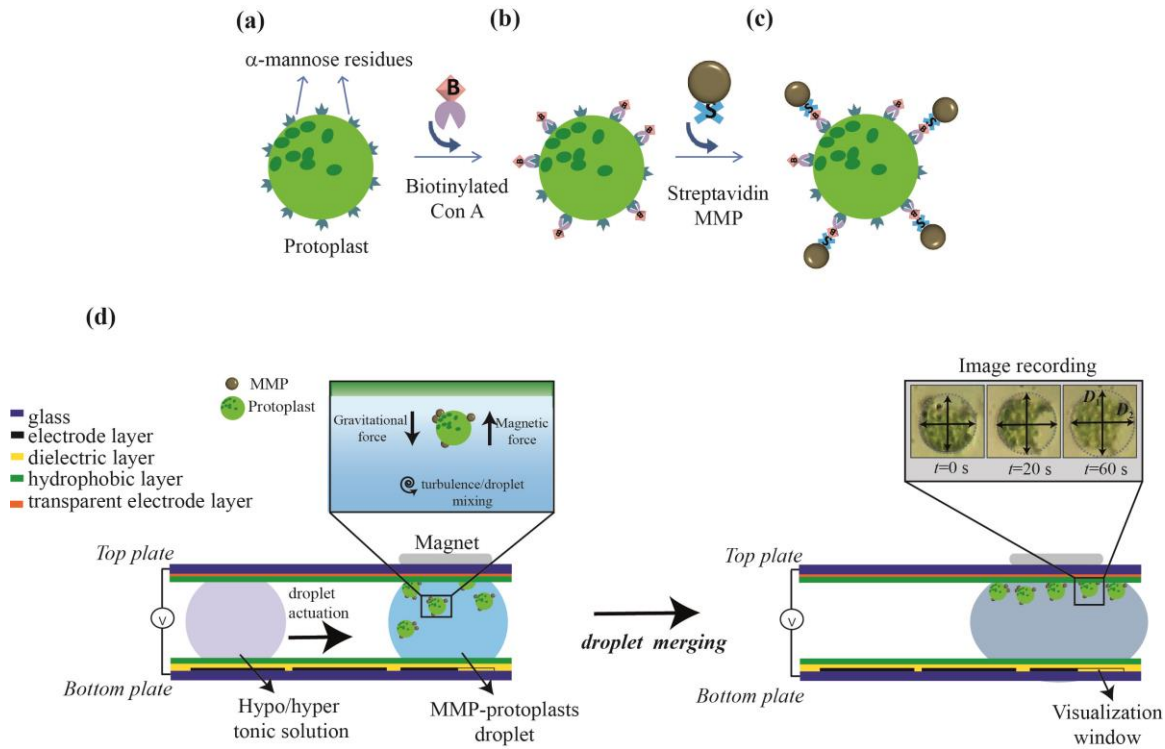


Figure 1. Flowchart illustrating Concanavalin A (ConA)-magnetic microparticle (MMP) labelling of protoplasts. (a) Protoplasts with α -mannose residues displayed on the plasma membrane; (b) functionalization of protoplast residues with biotinylated ConA and (c) MMP labelling using streptavidin-biotin binding; (d) Schematic depicting on-chip treatment of protoplasts with hypo/hyper tonic solution and concurrent volume monitoring through an external digital camera followed by image analysis.

magnet (NeFeB, 5 mm diameter, 3 mm thickness, 6.86 N, Super magnete, Germany) placed above the top plate and resulting in immobilization of the magnetic particle-conjugated protoplasts (Fig. 1d). Next, the hypotonic droplet consisting of water was actuated and merged with the protoplasts droplet and the subsequent change in volume of the cells was recorded via the microscope mounted camera (respectively CKX41-Olympus, Japan and VX-5500-Microsoft, US). By means of DMF manipulations, an average of 7 protoplasts were treated and analysed in every field of view.

Recorded movies were processed using one frame per second with every protoplast serially using a freeware image analysis program (ImageJ, US National Institutes of Health, Bethesda, Maryland, USA). For calculating the cell volume, the protoplast shape was assumed to be a prolate spheroid [28] rather than a perfect sphere as it was observed that during the hypotonic treatment protoplasts did not always maintain a perfectly spherical shape but often grew in size in an ellipsoid way. By drawing an ellipse around individual protoplasts, the volumes ($1/6\pi D_1 D_2^2$) at the different time points were calculated by the measured major (D_1) and minor axis (D_2) of the fitted ellipse.

2.6 Calculation of water permeability coefficient (P)

To calculate the water permeability P , a model was developed and implemented. The mathematical formulation of hydraulic conductivity (L_v in $\text{m s}^{-1} \text{Pa}^{-1}$) can be expressed as:

205

$$206 \quad L_v = \frac{P \cdot V_w}{R \cdot T} \quad (1)$$

207

208 where P is the water permeability coefficient (m s^{-1}), V_w is the partial molar volume of water ($18 \times 10^{-6} \text{ m}^3 \text{ mol}^{-1}$), R is
 209 the universal gas constant ($8.314 \text{ J mol}^{-1} \text{ K}^{-1}$) and T corresponds to room temperature 293K. The volumetric flux of
 210 water ($\text{m}^3 \text{ s}^{-1} \text{ m}^{-2}$) through a permeable membrane can be written as:

211

$$212 \quad \phi_v = L_v \cdot \Delta \psi \quad (2)$$

213

214 where $\Delta \psi$ is the gradient in water potential over the membrane (Pa). The mass of water transported across the
 215 membrane is balanced by the volume change of the protoplast and can be written as:

216

$$217 \quad \rho \frac{dV}{dt} = -A \cdot \rho \cdot L_v \cdot \Delta \psi \quad (3)$$

218

219 with A (m^2), V (m^3) and ρ (kg m^{-3}) the protoplasts surface area, protoplast volume and density of water, respectively.
 220 The water potential is assumed to consist only of the osmotic potential, and according to Van't Hoff equation, for an
 221 external total solute concentration C_s (mol m^{-3}), the water potential can be calculated as:

222

$$223 \quad \psi = -RTC_s \quad (4)$$

224

225 The surface area of the protoplast changes with subsequent volume increase/decrease; however, in the previous
 226 studies [11] only the initial surface area has been considered (eq. (3)). If the protoplast shape is assumed to be a
 227 prolate spheroid with D_1 being the major and, D_2 and D_3 the minor axis, the change in volume of the protoplasts as a
 228 function of time can be written as

229

$$230 \quad \text{and} \quad \frac{d(\pi D_1 D_2^2)}{6dt} = -\frac{\pi}{2} D_2^2 \left(1 + \frac{D_1}{D_2 b} \sin^{-1} b \right) RT L_v (C_s - C_{int}) \quad (5)$$

231

$$232 \quad \text{where} \quad \begin{aligned} D_1 &\neq D_2 = D_3 \\ D_1 &> D_2 \end{aligned}$$

$$233 \quad \text{and} \quad b^2 = 1 - \frac{D_2^2}{D_1^2} \quad c > a$$

234 C_{int} and C_s are the internal and external total solute concentration (mol m^{-3}) respectively. Finally, from eq. (1), (2) and
 235 (5), eq. (6) was deduced in terms of water permeability coefficient as:

236

$$\frac{d(\pi D_1 D_2^2)}{6dt} = -\frac{\pi}{2} D_2^2 \left(1 + \frac{D_1}{D_2 b} \sin^{-1} b \right) P V_w (C_s - C_{int}) \quad (6)$$

238

239 The initial volume $V(0)$ and final volume $V(t)$ can be written as:

240

$$V(0) = \frac{4}{3} \pi \frac{D_1(0)}{2} \left(\frac{D_2(0)}{2} \right)^2 \quad (7)$$

$$V(t) = \frac{4}{3} \pi \frac{D_1(t)}{2} \left(\frac{D_2(t)}{2} \right)^2 \quad (8)$$

243

244 where $D_1(0)$, $D_2(0)$ and $D_1(t)$, $D_2(t)$ are values of D_1 and D_2 at time 0 and t , respectively. The concentration
 245 gradient across the plasma membrane will change with time t , while reaching the target concentration. The changing
 246 internal solute concentration $C_{int}(t)$ within the protoplast at time t can be calculated with respect to the initial internal
 247 concentration and volume changes as:

248

$$C_{int}(t) = \frac{C_{int}(0)V(0)}{V(t)} \quad (9)$$

250

251 The term $C_{int}(t)$ represents the gradual change of the initial internal solute concentration due to cellular volume
 252 changes. Also, during the on-chip merging of two droplets, proper mixing of droplets will require a finite amount of
 253 time. In order to include the delay in reaching the target concentration C_{target} in the droplet, an additional differential
 254 equation based on first order kinetics characterized by a rate constant (k_c) was introduced in the model:

255

$$\frac{dC_s}{dt} = k_c (C_s - C_{target}) \quad (10)$$

257

258 In our model we assumed that protoplast shape and aspect does not change over time. Hence to obtain two
 259 differential equations for the two evolving axis, an additional constant k was introduced in the model which was
 260 defined as

$$k = \frac{D_1}{D_2} \quad (11)$$

262 This assumption was based on the fact that from our measurements it appeared that the aspect of the protoplast does
 263 not change over time. Hence, from eq. (6)-(11), the rate of change of the major and minor axis can be deduced as:

264

$$\frac{d(D_1)}{dt} = - \left(1 + \frac{k^2}{\sqrt{k^2 - 1}} \sin^{-1} \sqrt{1 - \frac{1}{k^2}} \right) P V_w \left(C_s - C_{int}(0) \frac{6V(0)k^2}{\pi D_2^3} \right) \quad (12)$$

$$\frac{d(D_2)}{dt} = - \left(\frac{1}{k} + \frac{k}{\sqrt{k^2 - 1}} \sin^{-1} \sqrt{1 - \frac{1}{k^2}} \right) PV_w \left(C_s - C_{int}(0) \frac{6V(0)}{\pi k D_2^3} \right) \quad (13)$$

Using eq. (12-13), permeability coefficient value (P) is determined. The model simulates the change over time of D_1 and D_2 on the basis of the changing internal solute concentration $C_{int}(t)$ within a protoplast. C_{int} is an unknown and dynamic value which is in turn calculated from the measured change of volume over time using eq. (7-10). The changing C_{int} is further used for simulating major and minor axis values that can best model the monitored data. The developed model (eq. (8-13)) was implemented and model parameters (P , $D_1(t)$ and $D_2(t)$) were estimated using OptiPa [29], a dedicated optimisation tool that was developed for use with Matlab (Matlab R2011b, The MathWorks, Inc., Natick, MA, USA). Model parameters were estimated on the basis of least-square non-linear optimization. To take into account the reliability of subsequent measured points, a weighting vector was introduced. As some time series showed clear artefact towards the end of the measured data, the weighting was used to down weight the influence of latter measurements, as compared to earlier measurements, on the calculated P .

3. Results and Discussion

3.1 Magnetic microparticle labelling of protoplasts

The non-adhering nature of suspension cells sets a major limitation in monitoring and tracking the responses of single isolated cells. Hence immobilization strategies are required to effectively limit the spatial motility of such cells in three dimensions. We choose magnetic labelling as a strategy to anchor cells on a fixed position. Due to the unavailability of adequate antibodies which could conjugate with epitopes located on the exterior of the *A. Thaliana* plasma membrane, we looked for a versatile linker molecule with applicability over a wide range of suspension cell types. Concanavalin A is a protein molecule, that selectively recognizes α -linked mannose present as part of a core oligosaccharide in many serum and membrane glycoproteins. It has been demonstrated in the literature for isolating DNA, proteins and various cell types [25,26,30,31]. Here, for coupling streptavidin coated MMP to protoplasts, biotinylated ConA was chosen as a linker molecule. Protoplast were isolated from *A. thaliana* plants (Fig. 2a) and functionalised with biotinylated ConA. During the functionalization a reduction in the number of cells was observed after incubation with ConA concentrations higher than $10 \text{ ng } \mu\text{L}^{-1}$, suggesting a negative effect of ConA on cell integrity, which caused protoplasts to burst (Fig. 2b).

Toxic effects of ConA have been previously described in literature and are due to the activation of intracellular pathways that leads to apoptosis, possibly after ConA internalization [32,33]. However in the presented experiments, this toxic effect of ConA was negligible at concentrations lower than $10 \text{ ng } \mu\text{L}^{-1}$ which was thus defined as the highest dosage to be used in further experiments. ConA treatment of protoplasts also had an effect on the clustering of cells, defined as two or more cells physically interacting (Fig. 2c). Clustering became more prominent at higher ConA concentrations with about 70% of the cells clustered at the highest concentration tested (Fig. 2d). Such effect is not surprising as it is known that ConA is a multivalent molecule and can bind to more than one α -linked mannose group at the time hence forming bridges between cells [33–35]. For the purposes of this work, overcrowding of cells needed to be avoided as it would hinder accurate monitoring of protoplasts morphology during

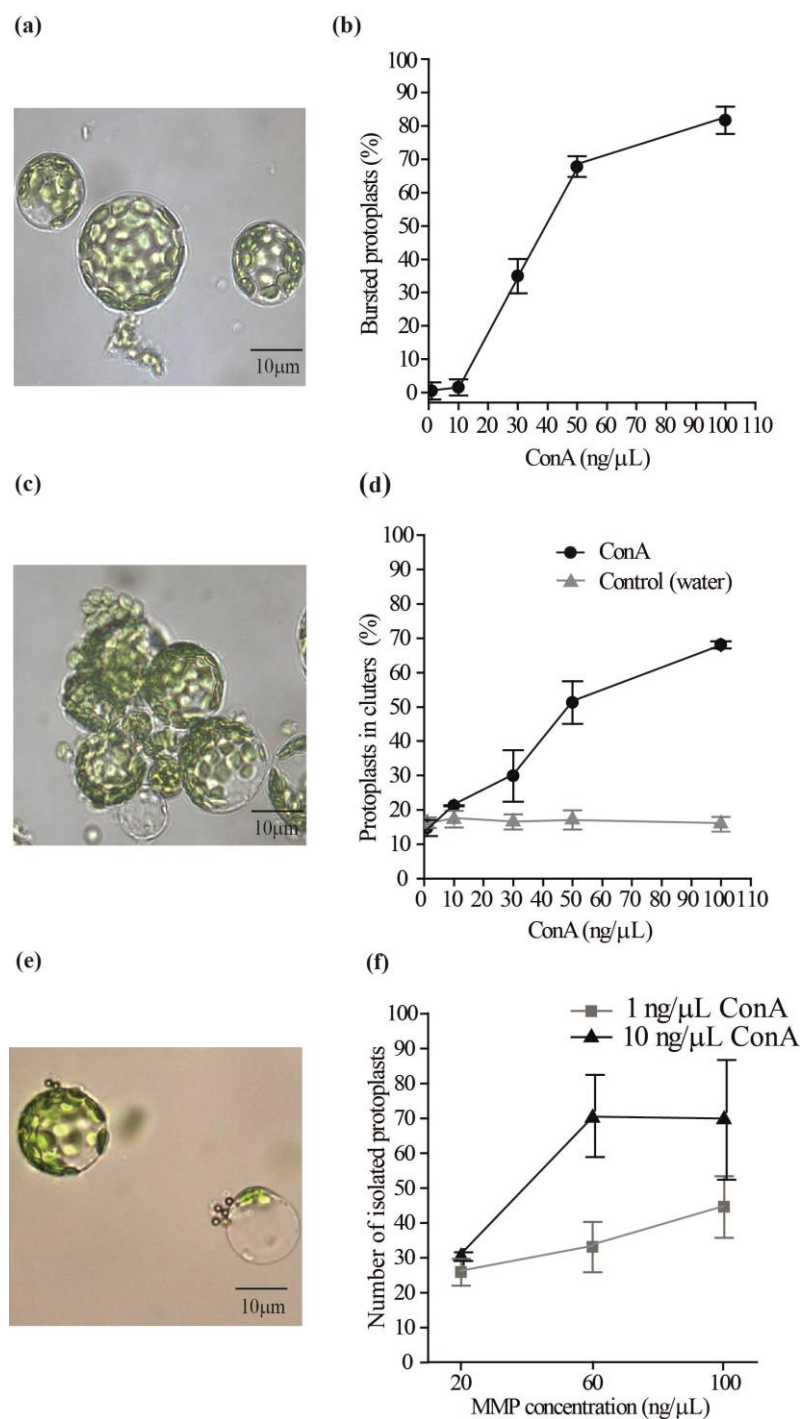


Fig.2. ConA labelling and MMP-protoplast isolation (a) Isolated protoplasts before incubation with ConA; (b) toxic effect of ConA expressed as percentage of protoplasts that burst upon ConA treatment relative to the initial cell number. Error bars indicate standard errors for three replicates; (c) typical cluster of protoplasts forming after ConA labelling; (d) effect of ConA treatment on protoplasts clustering expressed as percentage of cells in clusters (consisting of 2 or more cells) relative to the total viable protoplasts isolated at different ConA concentration. The control samples are protoplasts treated with equivalent volume of the solvent in which ConA is dissolved (water). Error bars indicate standard errors for three replicates. (e) Bright field image of protoplasts conjugated with MMP; (f) protoplast isolation at selected ConA concentrations and MMP concentrations. Error bars indicate standard error for four replicates.

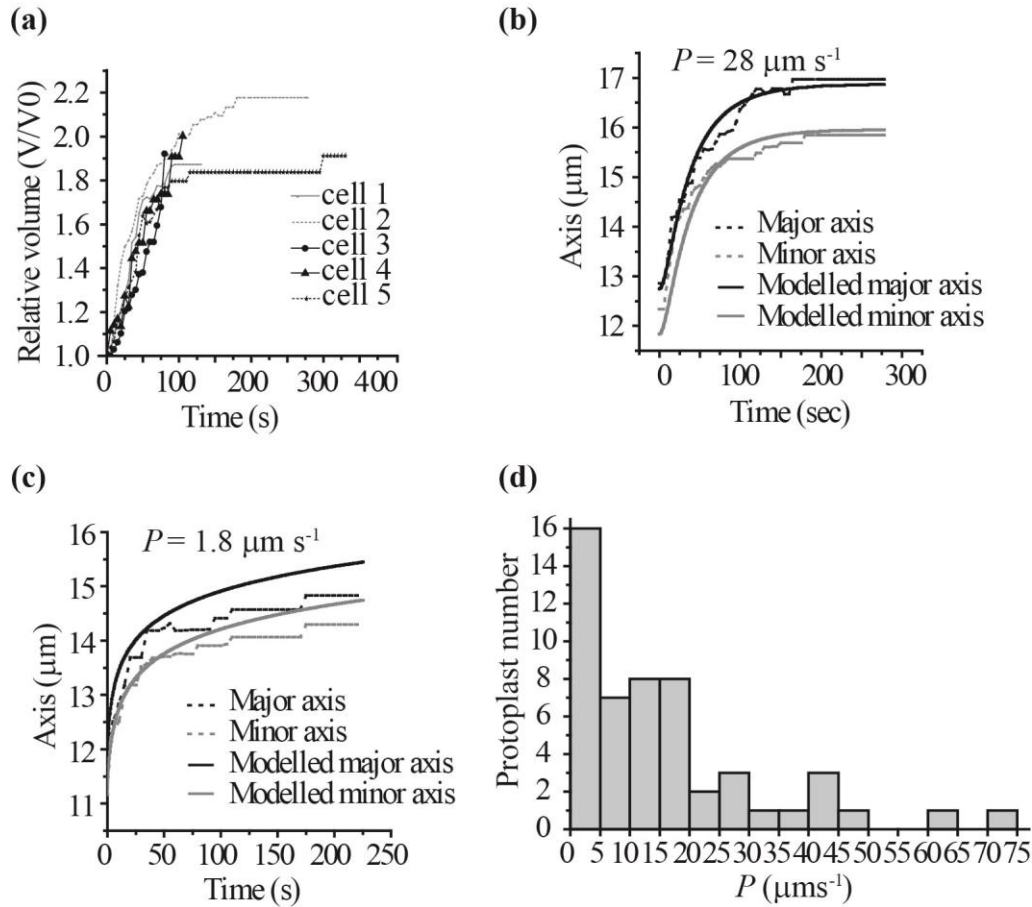


Fig. 3. Volume increase, water permeability calculations and data modelling. (a) Volume changes of 5 individual protoplasts treated at $\Delta\psi=0.99$ MPa and simultaneously monitored; (b) typical diameter changes modelled for a single protoplast treated at $\Delta\psi=0.99$ MPa; (c) diameter changes of a protoplast treated at $\Delta\psi=0.99$ MPa with stretched plasma membrane and down weighting of subsequent data points; (d) distribution of P values measured for 50 single protoplasts treated at $\Delta\psi=0.70$ MPa and $\Delta\psi=0.99$ MPa on the DMF chip.

the water permeability measurements, thereby compromising the quality of measurements on the DMF chip. Based on these considerations and the preliminary experiments, 1-10 ng μL^{-1} ConA was selected as the working range for the next experiments. The second step of the procedure required incubation of biotinylated ConA protoplasts with streptavidin coated MMP (Fig. 2e).

To determine the optimal concentration of MMP to be used for efficient protoplasts isolation but at the same to avoid excessive residual MMP presence in the final preparation, protoplasts functionalized either with 1 ng μL^{-1} or 10 ng μL^{-1} of ConA were incubated with different concentrations of MMPs and the number of isolated protoplasts was valuated after several washing steps (Fig. 2f). Among the different conditions tested, the combination of 10 ng μL^{-1} ConA and 60-100 ng μL^{-1} MMP delivered the highest number of isolated protoplast. For the condition 10 ng μL^{-1} ConA (Fig. 2f black curve), it was observed that the number of retrieved protoplasts initially increased with increasing MMP concentrations and reached plateau at 60 ng μL^{-1} MMP, suggesting a saturation of the exposed biotinylated tags on the cell surface. Moreover, to minimize the effect of MMPs on the protoplast integrity, the

average number of MMPs bound on the protoplast membrane was counted. At $60 \text{ ng } \mu\text{L}^{-1}$ MMP, most protoplasts had less than four MMPs attached to their surface. In conclusion, $10 \text{ ng } \mu\text{L}^{-1}$ ConA and $60 \text{ ng } \mu\text{L}^{-1}$ MMP were selected as working concentrations and used in all other experiments. The isolated protoplasts were then used for conducting water permeability measurements on the DMF chip.

3.2 Water permeability measurements using DMF chip

In the presented experiments, protoplasts were exposed either to a relatively moderate or extreme hypo-osmotic condition corresponding to an osmotic pressure change ($\Delta\psi$) of 0.70 MPa and 0.99 MPa, and to a relatively moderate or extreme hyper-osmotic stress condition corresponding to an osmotic pressure change ($\Delta\psi$) of -1.21 MPa and -2.4 MPa, respectively. Protoplasts were initially immobilized using an external magnet on the DMF chip, which contained a specifically designed transparent visualization window. Using the EWOD actuation principle, a droplet with suspended protoplasts was merged with a hypotonic droplet (water) or hypertonic droplet (buffer) (Fig.1d) which resulted in the transportation of water from the external solution towards the protoplast interior or from the protoplast interior towards the external solution. This water transport over the membrane resulted in an increase or decrease of the protoplast volume and consequently a change in volume. In Fig. 3a, typical volumetric changes are shown for five single protoplasts that were simultaneously treated at a $\Delta\psi$ of 0.99 MPa and monitored over a period of 360 s (see supplementary information for other tested conditions).

For the on-chip monitored protoplasts, the volume increased in a non-linear way with time before reaching a final constant value. At the most extreme hypotonic condition tested ($\Delta\psi=0.99 \text{ MPa}$), 55% of the tested protoplasts did burst after an initial volume increase (Fig. 3a), whereas for the moderate hypotonic test condition ($\Delta\psi=0.70 \text{ MPa}$), this phenomenon occurred in 10% of the tested protoplast (supplementary information). This reveals a low tolerance of certain protoplasts towards the abrupt change in the external osmotic condition. One of the possible reasons could be that due to the rapid influx of water in the protoplasts, the plasma membrane gets excessively stretched, finally leading to the lysis of the protoplasts [36]. Protoplasts when treated with hypertonic conditions ($\Delta\psi=-1.21 \text{ MPa}$ and $\Delta\psi=-2.44 \text{ MPa}$) started to loose water molecules that lead to shrinkage of protoplasts. We observed that the shrinking phenomenon was highly non-uniform in all the directions, (supplementary information) which lead to change in protoplast shape over time and the model could no longer be applied on the protoplasts. Also extreme hypertonic treatments could lead to implosion and hence death of protoplasts which could not be detected clearly during the experiments. Hence we decided to evaluate only hypotonic conditions because the analysis was more suitable for the developed modeled. After the droplet merging step, the volume changes started with a short delay indicating a finite delay in reaching a uniform concentration in the droplet. This delay was considered in the model for calculating P values (see model, eq. (10)). The volume changes were calculated from the measured axis changes (D_1 and D_2). As depicted in Fig. 3b, the two axis lengths showed a non-linear trend which stabilized once the external and internal concentration were equal. The presented results illustrate the suitability of DMF chips for the treatment of multiple non-adhering cells with different stimuli and simultaneously monitoring their response at a single cell resolution. The data also showed that on-chip merging of droplets was effective in changing the osmolarity of the final droplet as the kinetics of the volumetric changes observed are in agreement with those

obtained by traditional methods and reported in literature [36]. Next, the rates of major and minor axis change were used for calculating the water permeability coefficients of every single protoplasts.

3.3 Water permeability coefficient calculation (P) for protoplasts treated on DMF chip

As a next step, P values were estimated for every single individual protoplast by fitting the model deduced from eq. (8-13) to the experimental data consisting of minor and major axis length using OptiPa (see Materials and Methods for a detailed explanation) [10]. For P calculations, a delay factor was included in the model by introducing a rate constant (k_c) describing the changes in the external solute concentration until the desired target concentration is reached after the droplet merging has completed. The delay factor (k_c) was initially estimated based on a range of protoplasts and the average k_c was used as a constant for all the protoplast tested at different conditions. In the absence of this delay factor a less good fit was obtained. We observed that for certain protoplasts, the model could not well describe all of the axis change data. The poor fitting could be explained by plasma membrane stretching where protoplasts started leaking certain solute molecules into the medium altering the osmotic gradient across the plasma membrane. To take into account the potentially increasing inaccuracy of data collected from all protoplast including stretched protoplasts, the contribution of consecutive measurements to the overall model fit was increasingly down-weighted. In this way most emphasis was given to the initial readings that are expected to be the most accurate ones. The down-weighting was hence applied to all the protoplasts analysed on the DMF platform. In Fig. 3b, the two experimental curves (dashed lines) reflect the typical changes over time in the major and minor axis occurring in one single isolated protoplast treated at an osmotic pressure change of 0.99 MPa. The superimposition of the experimental data (dashed line) and the modelled theoretical data (solid line) showed good fitting, suggesting that leaking due to plasma membrane stretching did not occur in this protoplast. In Fig.3c instead, a proper fit between the experimental data (dashed line) and the modelled theoretical data (solid line) could not be obtained, suggesting over stretching of the plasma membrane of this single isolated protoplast. Thanks to the down-weighting factor, the model could still be successfully applied to the overstretched protoplast and a proper value for the permeability coefficient (P) could be estimated as the information for estimating P is mainly contained in the first dynamic part of the curve where the model fits the cell size data well. These results confirm the validity of the described model and demonstrate the suitability of the DMF chip for performing this type of analysis.

By means of DMF droplet manipulations, 50 single *A. Thaliana* protoplasts were successfully analysed and individual P values were obtained ranging from $1 \mu\text{m s}^{-1}$ to $75 \mu\text{m s}^{-1}$ (Fig. 3d). To compare the distribution of the 50 P values obtained for the protoplasts treated with two hypotonic conditions, we conducted Mann-Whitney U test. According to this nonparametric test (p-value = 0.2548 was obtained), it could be concluded that the *Permeability coefficient values* were not statistically different in the two hypotonic treatments and could be pooled. Large variations in P values of populations of cells are commonly observed in these types of experiments ($1.25\text{-}540 \mu\text{m s}^{-1}$) [37], which mostly reflect the existing variations in aquaporin expression or activity within plasma membranes of different cells [38]. The P values obtained are thus in line with the values presented in the literature [37] and perfectly illustrate the heterogeneity present within a population of cells when exposed to the same stimuli.

This study confirms that DMF chip is an efficient platform for generating the steep gradient steps necessary for the

implementation of water potential studies at a single cell level and it further validates the usefulness of the illustrated immobilization strategy, which successfully retains small non-adhering cells during the rapid external solution exchange. Furthermore, this approach allows a substantial increase in the throughput of the analysis as an average of seven cells can be monitored and followed simultaneously within a single field of view.

4. Conclusion

We have described in this article a proof of concept for the analysis of naturally non-adhering plant cells that combines magnetic microparticle labelling and DMF chip technology. The presented system takes advantage of the easy manipulation of particles and cells provided by the use of DMF chips. Furthermore, DMF chips are particularly suited for the handling of inherently delicate cells such as protoplasts, which are prone to breakage due to the absence of a cell wall. This approach allows for (i) a substantial increase in the throughput of water permeability measurements on single protoplasts cells and (ii) delivers *P* values comparable to those reported in literature, confirming the suitability of the approach. Although the magnetic particle-labelling of cells was performed off-chip in this study, the use of DMFs offers the prospect of automating all sample preparation steps, such as the functionalization of magnetic particles, as these ones can be extracted from a first droplet and re-incubated with new reagents or with a cell suspension to fully automate all experimental operations [39]. The platform described here provides an answer to the need of immobilizing those types of cells that do not adhere to the substrates for analysis at the single cell level and introduces automation in the field of water potential studies. Keeping our focus on single cell analysis, we speculate that this approach can be easily applied to a vast range of biological applications.

Acknowledgements

The research leading to these results has received funding from the European Commission's Seventh Framework Programme (FP7/2007-2013) under the grant agreement BIOMAX (project n° 264737), from the Fund for Scientific Research Flanders (FWO G.0997.11, FWO G.0645.13), and from the KU Leuven (IOF-Knowledge platform "Atheromix", IDO-project "Cellphinder" (10/012), DBOF mandate PT 10/024, and OT-project 13/058 and 12/055).

References

- [1] M.J. Chrispeels, N.M. Crawford, J.I. Schroeder, Proteins for transport of water and mineral nutrients across the membranes of plant cells., *Plant Cell*. 11 (1999) 661–76.
- [2] M.T. Conner, A.C. Conner, C.E. Bland, L.H.J. Taylor, J.E.P. Brown, H.R. Parri, R.M. Bill, Rapid aquaporin translocation regulates cellular water flow: mechanism of hypotonicity-induced subcellular localization of aquaporin 1 water channel., *J. Biol. Chem.* 287 (2012) 11516–25.
- [3] M. Chrispeels, C. Maurel, Aquaporins: the molecular basis of facilitated water movement through living plant cells?, *Plant Physiol.* 100 (1994) 9–13.
- [4] P. Agre, Aquaporin water channels in kidney, *J. Am. Soc. Nephrol.* 11 (2000) 764–777.
- [5] P.F. Scholander, E.D. Bradstreet, E.A. Hemmingsen, H.T. Hammel, Negative hydrostatic pressure can be measured in plants, *Science* (80-.). 148 (1965) 339–46.

- 426 [6] D. Hüskes, E. Steudle, U. Zimmermann, Pressure probe technique for measuring water relations of cells in higher
427 plants., *Plant Physiol.* 61 (1978) 158–63.
- 428 [7] D. Tomos, The plant cell pressure probe, *Biotechnol. Lett.* 22 (2000) 437–442.
- 429 [8] R. Zhang, A. Verkman, Water and urea permeability properties of *Xenopus* oocytes: expression of mRNA from toad
430 urinary bladder, *Am. J. Physiol. Cell Physiol.* 260 (1991) C26–C34.
- 431 [9] T. Ramahaleo, R. Morillon, J. Alexandre, J. Lassalles, Osmotic Water Permeability of Isolated Protoplasts. Modifications
432 during Development, *Plant Physiol.* 119 (1999) 885–896.
- 433 [10] S. Suga, M. Murai, T. Kuwagata, M. Maeshima, Differences in aquaporin levels among cell types of radish and
434 measurement of osmotic water permeability of individual protoplasts., *Plant Cell Physiol.* 44 (2003) 277–86.
- 435 [11] M. Moshelion, N. Moran, F. Chaumont, Dynamic changes in the osmotic water permeability of protoplast plasma
436 membrane, *Plant Physiol.* 135 (2004) 2301–2317.
- 437 [12] X. Wang, S. Chen, M. Kong, Z. Wang, K.D. Costa, R. A. Li, D. Sun et al., Enhanced cell sorting and manipulation with
438 combined optical tweezer and microfluidic chip technologies., *Lab Chip.* 11 (2011) 3656–62.
- 439 [13] J. Enger, M. Goksör, K. Ramser, P. Hagberg, D. Hanstorp, Optical tweezers applied to a microfluidic system., *Lab Chip.*
440 4 (2004) 196–200.
- 441 [14] H. Zhang, K.K. Liu, Optical tweezers for single cells, *Interface.* 5 (2008) 671–690.
- 442 [15] D. Witters, K. Knez, F. Ceyssens, R. Puers, J. Lammertyn, Digital microfluidics-enabled single-molecule detection by
443 printing and sealing single magnetic beads in femtoliter droplets., *Lab Chip.* 13 (2013) 2047–54.
- 444 [16] S. Srigunapalan, I.A. Eydelnant, C.A. Simmons, A.R. Wheeler, A digital microfluidic platform for primary cell culture
445 and analysis., *Lab Chip.* 12 (2012) 369–75.
- 446 [17] D. Witters, N. Vergauwe, S. Vermeir, F. Ceyssens, S. Liekens, R. Puers, J. Lammertyn., Biofunctionalization of
447 electrowetting-on-dielectric digital microfluidic chips for miniaturized cell-based applications., *Lab Chip.* 11 (2011)
448 2790–4.
- 449 [18] I. Barbulovic-Nad, S.H. Au, A.R. Wheeler, A microfluidic platform for complete mammalian cell culture., *Lab Chip.* 10
450 (2010) 1536–42.
- 451 [19] G.J. Shah, A.T. Ohta, E.P.-Y. Chiou, M.C. Wu, C.-J.C.J. Kim, EWOD-driven droplet microfluidic device integrated with
452 optoelectronic tweezers as an automated platform for cellular isolation and analysis., *Lab Chip.* 9 (2009) 1732–9.
- 453 [20] D. Bogojevic, M.D. Chamberlain, I. Barbulovic-Nad, A.R. Wheeler, A digital microfluidic method for multiplexed cell-
454 based apoptosis assays., *Lab Chip.* 12 (2012) 627–34.
- 455 [21] S.H. Au, S.C.C. Shih, A.R. Wheeler, Integrated microfluidic platform for culture and analysis of bacteria, algae and yeast.,
456 *Biomed. Microdevices.* 13 (2011) 41–50.
- 457 [22] I. Barbulovic-Nad, H. Yang, P.S. Park, A.R. Wheeler, Digital microfluidics for cell-based assays., *Lab Chip.* 8 (2008)
458 519–26.
- 459 [23] S.-D. Yoo, Y.-H. Cho, J. Sheen, Arabidopsis mesophyll protoplasts: a versatile cell system for transient gene expression
460 analysis., *Nat. Protoc.* 2 (2007) 1565–72.
- 461 [24] Y.-C. Lee, G. Block, H. Chen, E. Folch-Puy, R. Foronjy, R. Jalili, C. B. Jendresen, M. Kimura, E. Kraft, S. Lindemose,
462 J. Lu, T. McLain, L. Nutt, S. R.-Garcia, J. Smith, A. Spivak, M. L. Wang, M. Zanic, S. H. Lin, One-step isolation of

- 463 plasma membrane proteins using magnetic beads with immobilized concanavalin A., *Protein Expr. Purif.* 62 (2008) 223–
464 9.
- 465 [25] I. Safarik, M. Safariková, Use of magnetic techniques for the isolation of cells., *J. Chromatogr. B. Biomed. Sci. Appl.*
466 722 (1999) 33–53.
- 467 [26] I. Dörr, S. Miltenyi, F. Salamini, H. Uhrig, Selecting somatic hybrid plants using magnetic protoplast sorting, *Nat.*
468 *Biotechnol.* 12 (1994) 511–515.
- 469 [27] N. Vergauwe, D. Witters, F. Ceyskens, S. Vermeir, B. Verbruggen, R. Puers, J. Lammertyn, A versatile electrowetting-
470 based digital microfluidic platform for quantitative homogeneous and heterogeneous bio-assays, *J. Micromechanics*
471 *Microengineering.* 21 (2011) 054026.
- 472 [28] M. Maeda, G.A. Thompson, On the mechanism of rapid plasma membrane and chloroplast envelope expansion in
473 *Dunaliella salina* exposed to hypoosmotic shock., *J. Cell Biol.* 102 (1986) 289–97.
- 474 [29] M.L.A.T.M. Hertog, B.E. Verlinden, J. Lammertyn, B.M. Nicolaï, OptiPa, an essential primer to develop models in the
475 postharvest area, *Comput. Electron. Agric.* 57 (2007) 99–106.
- 476 [30] J. Porter, R. Pickup, C. Edwards, Evaluation of flow cytometric methods for the detection and viability assessment of
477 bacteria from soil, *Soil Biol. Biochem.* 29 (1997) 91–100.
- 478 [31] J.S. Tkacz, J.O. Lampen, Wall replication in *saccharomyces* species: use of fluorescein-conjugated concanavalin A to
479 reveal the site of mannan insertion., *J. Gen. Microbiol.* 72 (1972) 243–7.
- 480 [32] U. Rutishauser, L. Sachs, Receptor mobility and the mechanism of cell-cell binding induced by concanavalin A, *Proc.*
481 *Natl. Acad. Sci. U. S. A.* 71 (1974) 2456–2460.
- 482 [33] J.-C. Currie, S. Fortier, A. Sina, J. Galipeau, J. Cao, B. Annabi, MT1-MMP down-regulates the glucose 6-phosphate
483 transporter expression in marrow stromal cells: a molecular link between pro-MMP-2 activation, chemotaxis, and cell
484 survival., *J. Biol. Chem.* 282 (2007) 8142–9.
- 485 [34] U. Rutishauser, L. Sachs, Receptor mobility and the mechanism of cell-cell binding induced by concanavalin A, *Protoc.*
486 *Nat.* 71 (1974) 2456–2460.
- 487 [35] A. Sina, S. Proulx-Bonneau, A. Roy, L. Poliquin, J. Cao, B. Annabi, The lectin concanavalin-A signals MT1-MMP
488 catalytic independent induction of COX-2 through an IKKgamma/NF-kappaB-dependent pathway., *J. Cell Commun.*
489 *Signal.* 4 (2010) 31–8.
- 490 [36] A. Sommer, G. Mählknecht, G. Obermeyer, Measuring the osmotic water permeability of the plant protoplast plasma
491 membrane: implication of the nonosmotic volume., *J. Membr. Biol.* 215 (2007) 111–23.
- 492 [37] R. Morillon, M.J. Chrispeels, The role of ABA and the transpiration stream in the regulation of the osmotic water
493 permeability of leaf cells., *Proc. Natl. Acad. Sci. U. S. A.* 98 (2001) 14138–43.
- 494 [38] C.M. Niemietz, S.D. Tyerman, Characterization of Water Channels in Wheat Root Membrane Vesicles., *Plant Physiol.*
495 115 (1997) 561–567.
- 496 [39] A.H.C. Ng, K. Choi, R.P. Luoma, J.M. Robinson, A.R. Wheeler, Digital microfluidic magnetic separation for particle-
497 based immunoassays., *Anal. Chem.* 84 (2012) 8805–12.

498 Biographies

499 **Phalguni Tewari** was born in Lucknow (India) in 1987. She received the degree of bachelors and masters in
500 Nanotechnology from Amity University, Noida in 2010. For her master thesis, she focused on validation of HIV

501 nucleocapsid proteins interaction with various human cellular proteins. She is doing a PhD on the use of Digital
502 microfluidic platform for conducting single cells analysis in a project of the division of Mechatronics, Biostatistics
503 and Sensors (MeBioS) of the Biosystems Department at KU Leuven.

504 **Federica Toffalini** holds an MSc in Biotechnology and a PhD in Biomedical Sciences obtained at the Universite
505 Catholique de Louvain, Belgium. Her PhD work focused on the elucidation of molecular mechanisms underlying the
506 development of chronic leukemia caused by oncogenic forms of receptor tyrosine kinases. She next joined the
507 Biosensors group within the division of Mechatronics, Biostatistics and Sensors (MeBioS) of the Biosystems
508 Department at KU Leuven as a postdoctoral fellow. Her research focus includes cell-based applications of digital
509 microfluidic systems.

510 **Daan Witters** was born in Herk-de-Stad, Belgium, in 1986. He received his BS and MS in bio-engineering from the
511 KU Leuven, Leuven, Belgium in 2009. His master thesis was in the field of enzymatic assays performed on
512 microfluidic systems. He obtained his PhD at KU Leuven in October 2013 and his research interests concern the
513 design and application of digital microfluidic systems for performing high-throughput bio-assays and miniaturized
514 materials synthesis.

515 **Steven Vermeir** was born in Dendermonde (Belgium), in 1980. He received the degree of MS in biological
516 engineering from the KU Leuven, Belgium in 2003. In 2004, he became research assistant at the MeBioS-division
517 (KU Leuven) investigating miniaturized bioanalytical systems for the quantification of the most important taste
518 components in fruit and vegetables. He received his PhD in Bioscience Engineering in 2008. After that, he was a
519 research fellow of the FWO, exploring digital lab-on-a-chip technology as a novel analysis platform for single cell
520 studies.

521 **Filip Rolland** holds a MSc in Biology and obtained a PhD in Biology at KU Leuven in 2000. After his post-doctoral
522 training at Massachusetts General Hospital and Harvard University, USA (2001-2003) and KU Leuven (2003-2008),
523 he was appointed professor in the section of Molecular Physiology of Plants and Micro-organisms at the department
524 of Biology. He heads the research group of Metabolic Signaling in the lab of Molecular Plant Biology, focussing on
525 the molecular mechanisms of sugar and energy signaling in yeast and plants.

526 **Maarten Hertog** obtained his MSc in Biology at the University of Utrecht (NL) and obtained his PhD in the Applied
527 Biological Sciences at KU Leuven (BE). As research manager computational plant biology at KU Leuven he is
528 responsible for various applied system biology projects in the area of postharvest biology integrating the various
529 research disciplines operating at the various control levels through kinetic modelling approaches. He is editor of four
530 books in the area of food modelling and is member of the editorial board of Postharvest Biology and Technology.

531 **Bart M. Nicolai** obtained a MSc in bioscience engineering from Gent University (Belgium) in 1986, and a MSc in
532 applied mathematics (1988) and PhD in bioscience engineering (1994) from the University of Leuven (Belgium). He
533 is now full professor at the latter institute. Since 2005 he is head of the division mechatronics, biostatistics and

sensors (MeBioS) of the biosystems department at the University of Leuven. In addition, he is responsible for coordinating the research in the Flanders Center of Postharvest Technology (VCBT), an experimental facility which was established as a public–private partnership between the K University of Leuven and the Association of Belgian Horticultural Auctions in 1997. His main research interests are postharvest biology and technology, heat and mass transfer, and fruit and vegetable quality with flavour in particular.

Robert (Bob) Puers received his Ph.D. in 1986 at the KULeuven, where he created the ESAT-MICAS clean room sensor laboratories. He is a European pioneer in the research on micromachining, MEMS and packaging, mainly for biomedical implantable systems. Recently, microfluidic, microhydraulic and optical MEMS based on polymers have been added to his research. He took major efforts to increase the impact of MEMS and Microsystems in both the international research community as well as in industry. He helped to launch three spin-off companies, ICSense, Zenso and MinDCet. Dr. Puers is also an IEEE and IoP fellow.

Annemie Geeraerd holds a MSc in Bioscience Engineering and obtained her PhD at the University of Leuven in 1999. During her postdoctoral appointment, she worked at the French Food Safety Agency (AFSSA, now ANSES). She was appointed as a research professor in 2006. Her main research interest are on the development and application of mathematical models for quality, safety and sustainability of the food chain, with special attention to computational cell biology models related with fruit quality. She is author or co-author of 100+ peer reviewed journal papers and is member of the editorial board of the *International Journal of Food Microbiology* and *Journal of Food Protection*.

Jeroen Lammertyn holds a MSc in Bioscience Engineering and a MSc in Biostatistics. He obtained his PhD in Bioscience Engineering at the University of Leuven in 2001. From 2002 to 2005 he worked as postdoctoral researcher and spent one year as a research associate at the Pennsylvania State University, USA. Since 2005 he is appointed Professor at KU Leuven. His main research interests involve bionanotechnology and more specifically biosensor development, bionanohybrid materials, micro- and nanofluidics and bio-assay development. He teaches in the Master programs of Bioscience Engineering and Nanoscience and Nanotechnology. He is author or co-author of 100+ peer reviewed research papers and over 120 conference papers, and acts as reviewer for many international journals.